Mitochondria Supply Membranes for Autophagosome Biogenesis during Starvation

Dale W. Hailey,[1,3] Angelika S. Rambold,[1] Prasanna Satpute-Krishnan,[1] Kasturi Mitra,[1] Rachid Sougrat,[1,4] Peter K. Kim,[2] and Jennifer Lippincott-Schwartz[1,*]

[1]The Eunice Kennedy Shriver National Institutes of Child Health and Human Development, 18 Library Drive, Bethesda, MD 20892, USA
[2]Cell Biology Program, The Hospital for Sick Children, Toronto, Ontario, Canada
[3]Present address: University of Washington, Seattle, WA, USA
[4]Present address: The King Faisel University, Dammam, Saudi Arabia
*Correspondence: lippincj@mail.nih.gov

SUMMARY

Starvation-induced autophagosomes engulf cytosol and/or organelles and deliver them to lysosomes for degradation, thereby resupplying depleted nutrients. Despite advances in understanding the molecular basis of this process, the membrane origin of autophagosomes remains unclear. Here, we demonstrate that, in starved cells, the outer membrane of mitochondria participates in autophagosome biogenesis. The early autophagosomal marker, Atg5, transiently localizes to punctae on mitochondria, followed by the late autophagosomal marker, LC3. The tail-anchor of an outer mitochondrial membrane protein also labels autophagosomes and is sufficient to deliver another outer mitochondrial membrane protein, Fis1, to autophagosomes. The fluorescent lipid NBD-PS (converted to NBD-phosphotidylethanolamine in mitochondria) transfers from mitochondria to autophagosomes. Photobleaching reveals membranes of mitochondria and autophagosomes are transiently shared. Disruption of mitochondria/ER connections by mitofusin2 depletion dramatically impairs starvation-induced autophagy. Mitochondria thus play a central role in starvation-induced autophagy, contributing membrane to autophagosomes.

INTRODUCTION

During starvation, many organisms retrieve nutrients via degradation of their own intracellular components. This process is termed macroautophagy, or simply autophagy—"self eating." Autophagy is initiated by formation of multilamellar organelles that engulf cytosol en masse. Lysosomes subsequently fuse with autophagosomes and deliver lysosomal proteases. Captured substrates are thereby degraded, and transporters and

permeases in the membrane move components released by catabolism back to the cytosol (Xie and Klionsky, 2007). Autophagy during starvation is utilized throughout the eukaryotic domain. S. cerevisiae autophagy mutants rapidly die when cells are deprived of nitrogen and carbon (Scott et al., 1996; Tsukada and Ohsumi, 1993), nitrogen-starved Arabadopsis thaliana autophagy mutants exhibit increased rates of leaf senescence and chlorosis (Doelling et al., 2002), and mice lacking autophagy die shortly after birth during the switch from placental nourishment to suckling (Kuma et al., 2004).

An important question regarding starvation-induced autophagosomes is where these organelles originate from. Nearly all proteins involved in inception and maturation of autophagosomes are cytosolic proteins that are recruited to membranes (Xie and Klionsky, 2007). Proteomic studies have identified peripheral proteins but not a clear signature of membrane origin (Overbye et al., 2007), and reports have implicated membrane contribution from disparate sources including the endoplasmic reticulum (ER), trans Golgi network (TGN) and mitochondria (Axe et al., 2008; Reggiori et al., 2005; Young et al., 2006). Electron microscopy (EM) tomography has revealed close apposition of ER and phagophore membranes, most apparent when phagophore maturation is blocked (Hayashi-Nishino et al., 2009; Ylä-Anttila et al., 2009). These studies implicate involvement of the ER in autophagy, but it remains unclear whether this is a specific form of autophagy–ER-phagy–or whether the ER contributes to all autophagosome formation (Reggiori and Tooze, 2009). Because different membranes have been implicated in autophagosome biogenesis, it is possible the membrane origin of autophagosomes is variable. Here, we investigate formation of starvation-induced autophagosomes and uncover a mechanism involving contribution from the outer membrane of mitochondria that occurs during starvation but not ER stress. We show mitochondrial-derived membranes are utilized during autophagy and that autophagosome formation is dependent on ER/mitochondria connections modulated by mitofusin2 (Mfn2). These connections likely replenish mitochondrial lipid utilized for autophagic growth. We further identify a lipid anchor sequence that allows transfer of proteins from mitochondria to autophagosomes.
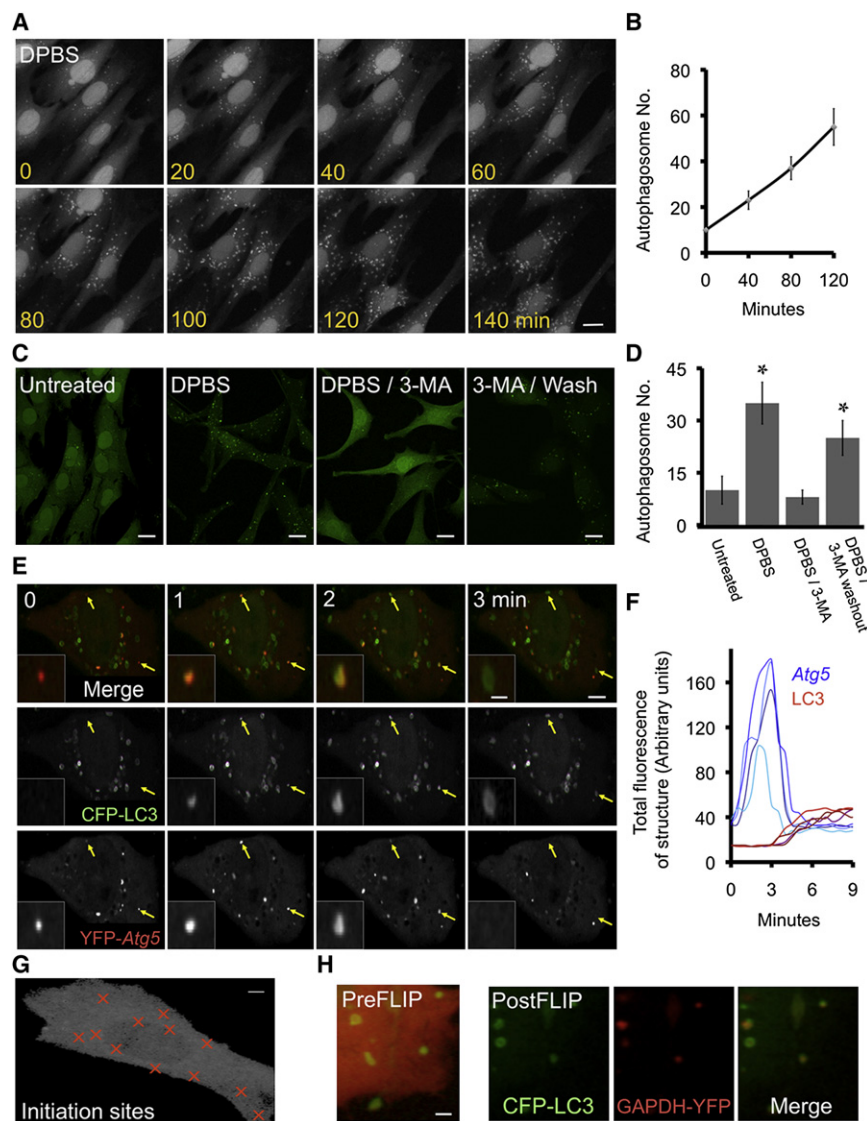
A

DPBS

0   20   40   60

80   100   120   140 min

B

Autophagosome No.

80
60
40
20
0

0   40   80   120

Minutes

C

Untreated | DPBS | DPBS / 3-MA | 3-MA / Wash

D

Autophagosome No.

45
30
15
0

Untreated   DPBS   DPBS / 3-MA   DPBS / 3-MA washout

E

0   1   2   3 min

Merge

CFP-LC3

YFP-*Atg5*

F

Total fluorescence of structure (Arbitrary units)

160
120
80
40
0

0   3   6   9

Minutes

Atg5
LC3

G

Initiation sites

H

PreFLIP | PostFLIP

CFP-LC3   GAPDH-YFP   Merge

Figure 1. Characterizing Formation of Starvation-Induced Autophagosomes

(A) Time-lapse imaging of starved NRK58B cells. CFP-LC3 positive structures rapidly proliferated during starvation. Note membrane recruitment of CFP-LC3 depleted cytosolic and nuclear pools. Growth media (time 0) was replaced with starvation media (subsequent panels). The scale bar represents 20 μm.

(B) Quantification of CFP-LC3 positive structures. Autophagosomes were counted in sequential frames and plotted as a function of time in starvation media. Data points show mean average of 20 cells. Error bars: 1 SD.

(C) Treatment with Class III PI(3) kinase inhibitor, 3-methyladenine (3-MA). Formation of CFP-LC3 structures required activity of the kinase. Identical wells were untreated, starved, or starved in the presence of 3-MA for 2 hr (three left panels). Starved cells treated with 3-MA were washed, incubated in DPBS and imaged 2 hr later (rightmost panel). 3-MA treatment abolished recruitment of CFP-LC3 to membranes and depletion of cytosolic and nuclear pools (2nd from right). Washout of 3-MA restored ability of cells to induce autophagosomes. The scale bar represents 20 μm.

(D) Quantification of 3-MA treatments (mean average of 20 cells $\pm$ 1 SD). Asterisk indicates treatment statistically different from untreated cells: p values < 0.001.

(E) Time-lapse imaging of NRK58B cells expressing YFP-*Atg5*. During starvation, YFP-*Atg5* punctae appeared, recruited CFP-LC3, and released YFP-Atg5. Arrows indicate two examples. Inset: zoom of autophagosome by lower right arrow. See also Movie S1. The scale bars represent 2 μm, inset ; and 10 μm, panel.

(F) Quantification of YFP-*Atg5* and CFP-LC3 signals in time-lapse frames. Dramatic accumulation of YFP-*Atg5* always preceded CFP-LC3 recruitment. YFP-*Atg5* persisted < 4 min and abruptly released.

(G) Mapping sites of autophagosome formation. Transient YFP-*Atg5* punctae that preceded CFP-LC3 recruitment were dispersed throughout the cytosol during starvation. The scale bar represents 5 μm.

(H) Identifying capture of cytosolic proteins in starvation-induced autophagosomes. Freely diffusing signal was depleted by repetitive photobleaching outside the panel. Photo-depletion revealed a GAPDH-YFP subpopulation captured in CFP-LC3 labeled structures. The scale bar represents 2 μm.

RESULTS

Characteristics of Starvation-Induced Autophagosomes

Starvation-induced autophagosomes were studied in a clonal Normal Rat Kidney cell line expressing cyan fluorescent protein (CFP) fused to LC3 (line NRK58B). LC3 (MAP1LC3, rat homolog of *S. cerevisiae* Atg8p) is a canonical autophagosome marker (Kabeya et al., 2000; Mizushima et al., 2004). Under replete growth conditions, CFP-LC3 was distributed between cytosolic and nuclear pools, with very little observed on autophagic membranes. Replacement of growth media with DPBS, HBSS or serum-free media induced a starvation response, and CFP-LC3 was recruited to autophagosomal membranes (Figure 1A).

Cells starved for 2 hr accumulated on average $\sim$50 CFP-LC3-labeled autophagic structures with very reproducible kinetics (Figure 1B). This response required Vps34/Beclin Class III PI3 kinase activity–an upstream event in autophagosome formation (Furuya et al., 2005). NRK58B cells starved in the presence of 10 mM 3-methyladenine (3-MA), an inhibitor of the kinase complex (Petiot et al., 2000), failed to recruit CFP-LC3 to punctae. Treated cells showed CFP-LC3 predominately in the cytoplasm or nucleus. Subsequent washout of 3-MA restored the ability to induce autophagy during starvation (Figures 1C and 1D).

Starvation induced autophagosomes also showed sequential recruitment of *Atg5* (mouse mAtg5) and LC3. *Atg5* marks sites of
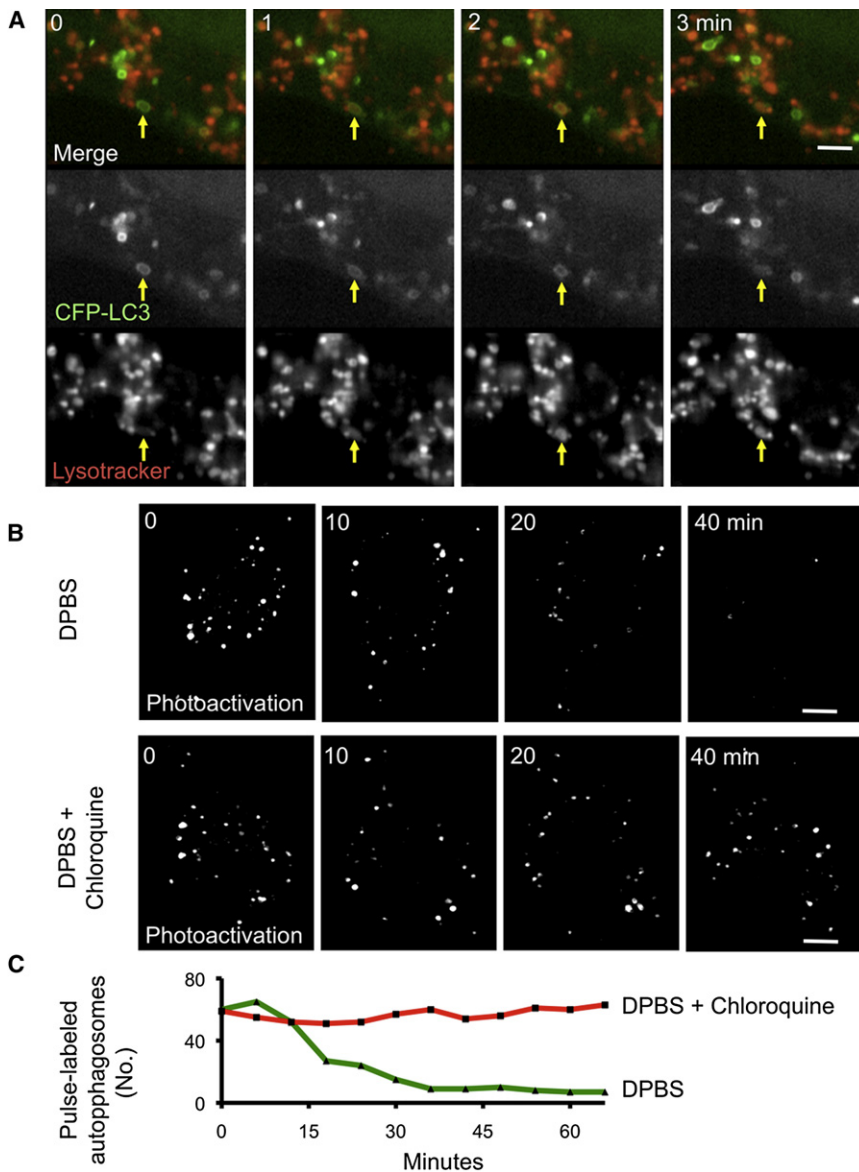
Figure 2. Characterizing the Fate of Starvation-Induced Autophagosomes

(A) Visualizing autophagosome/lysosome fusion. Starved NRK58B cells were labeled with a live-cell lysosomal marker. Vessicle fusion, accumulation of lysosomal marker and coincident loss of CFP-LC3 signal indicated fusion events between autophagosomes and lysosomes (arrow). See Movie S2.

(B) Visualizing turnover of autophagosomes by photo pulse-labeling. Following a 2 hr starvation, PAGFP-LC3 cells were photoactivated and depleted of cytosolic activated signal to pulse-label an existing autophagosome population (Top left panel). Live cell imaging revealed time dependent disappearance of the pulse-labeled population (top panels and Movie S3), which was blocked by addition of chloroquine.

(C) Quantification of the lifetime of the structures. Turnover of starvation-induced autophagosomes was rapid: $t_{1/2}$ of $\sim$25 min.

tae. These co-localized with lysosomal markers (not shown) or CFP-LC3 (Figure 1H), indicating autophagosomes with trapped cytosolic substrate. Autophagosomes in starved NRK58B were further characterized by LysoTracker labeling to visualize fusion between lysosomes and autophagosomes. Upon fusion, LysoTracker signal accumulated in CFP-LC3-labeled autophagosomes. Soon thereafter, CFP-LC3 signal from these structures was lost (Figure 2A; Movie S2).

The lifetime of starvation-induced autophagosomes was examined using photoactivatable GFP (PAGFP) (Patterson and Lippincott-Schwartz, 2002), which is invisible until activated by $\sim$400-nm irradiation. PAGFP-LC3 can be used to pulse-label and monitor an autophagosome population (Hailey and Lippincott-Schwartz, 2009). NRK cells expressing PAGFP-LC3 were starved, photoactivated, and monitored by live cell imaging. Starvation-induced autophagosomes exhibited near complete turnover within 40 min. Loss of PAGFP-LC3 signal was not due to photobleaching or release of PAGFP-LC3 from autophagosomes prior to lysosomal fusion, since loss of signal was blocked by treatment with chloroquine to inactivate lysosomal proteases and block fusion with lysosomes (Figures 2B and 2C; Movie S3) (Bjorkoy et al., 2005; Tasdemir et al., 2008).

Together these data indicate that starvation-induced autophagosomes in NRK58B cells are bona fide autophagosomes. They require Class III PI3Kinase activity and exhibit subsequent Atg5 and LC3 recruitment. These autophagosomes assemble at sites scattered throughout the cell, capture cytosolic substrates, and rapidly turn over in a lysosomal dependent fashion.

initial autophagosome formation and is necessary for recruitment of LC3 during starvation (Mizushima et al., 2001). We observed rapid accumulation of YFP-Atg5, followed by abrupt loss at punctae (Figure 1E; Movie S1 available online). YFP-Atg5 persisted for $\sim$3 min, and release always occurred concurrently with accumulation of CFP-LC3 (Figures 1E and 1F). We charted the intracellular locations of YFP-Atg5 and found that autophagosome assembly occurs at sites dispersed throughout the cell (Figure 1G).

Autophagosomes generated by starvation captured cytosolic components. Glyceraldehyde 3-phosphate dehydrogenase (GAPDH), an autophagy substrate (Hoyvik et al., 1991; Sneve et al., 2005), was expressed in nutrient-deprived NRK58B cells. Signal from freely diffusing GAPDH-YFP molecules was depleted by repetitively photobleaching a small region of cytosol to reveal non-diffusing subpopulations of GAPDH-YFP in punc-
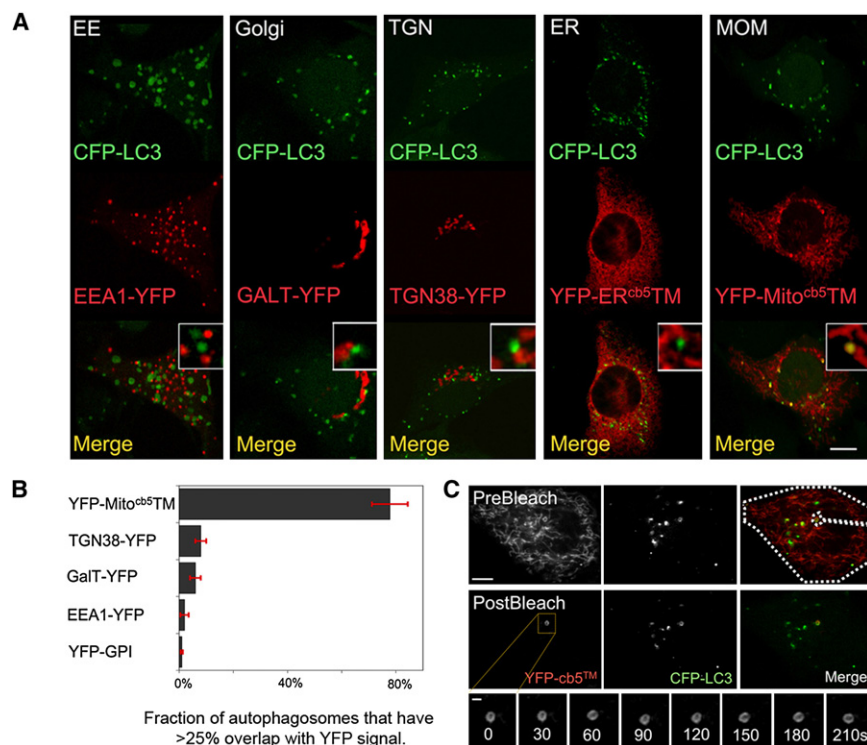
Figure 3. Evaluating Membrane-Targeted Markers for Transfer to Autophagosomes

(A) Expression of YFP-tagged membrane markers in starved NRK58B cells. Markers targeting membrane systems were expressed in NRK58B cells (left to right: early endosomal system, Golgi, TGN, ER, and mitochondrial outer membrane). Mitochondrial outer membrane marker, YFP-Mito^{cb5}TM, uniquely co-localized with autophagosomes. The scale bar represents 15 μm. (See also Figure S1 and Figure S2.)

(B) Quantification of CFP-LC3 overlap with membrane marker. For each marker, autophagosomes with greater than 25% CFP overlap with YFP were counted. This number was divided by the total number of autophagosomes to determine percent of autophagosomes that overlapped with the marker in each cell. Mean average of 20 cells is shown ± 1 SD. (See also Figure S3.)

(C) Stability of YFP-Mito^{cb5}TM on autophagosome membranes. YFP-Mito^{cb5}TM-positive autophagosomes were identified. YFP-Mito^{cb5}TM was subsequently bleached in the remainder of the cell (photobleached region indicated by hashed line, top right panel). YFP-Mito^{cb5}TM signal persisted on autophagosomes (time series in seconds, lower panel). The scale bars represent 10 μm, upper panel; and 1.5 μm, lower panel.

Identifying the Membrane Source of Starvation-Induced Autophagosomes

To identify membranes contributing to autophagosome formation, a battery of YFP-fusion proteins targeted to different intracellular organelles were expressed in NRK58B cells. We reasoned that if the membrane of an organelle was utilized for autophagosome formation, chimeric markers targeted to this membrane might be transferred to the induced autophagosomes. Markers tested included those for the Golgi apparatus, TGN, early endosomal system, plasma membrane, ER, and mitochondria. Tested ER markers included YFP fused to the targeting sequence of ER cytochrome b5, called YFP-ER^{cb5}TM. The targeting sequence of an isoform of cytochrome b5 (cb5) that labels the outer mitochondrial membrane tagged with YFP, called YFP-Mito^{cb5}TM was used to label mitochondria. This cb5 isoform has a shorter transmembrane region and positively charged residues at its distal C terminus than the cb5 isoform targeted to the ER–differences necessary and sufficient to target it specifically to the mitochondria outer membrane (Borgese et al., 2001; D'Arrigo et al., 1993; Lederer et al., 1983). YFP fusions to ER^{cb5}TM and Mito^{cb5}TM co-localized uniquely with ER and mitochondrial markers respectively. There was no YFP-ER^{cb5}TM signal in mitochondrial membranes, and no YFP-Mito^{cb5}TM signal in ER membranes (Figure S1). Most surveyed organelles revealed little or no overlap with CFP-LC3-positive autophagosomes (Figures 3A and 3B). For ER markers including YFP-ER^{cb5}TM, regions of low ER density showed no overlap with CFP-LC3 (Figure 3A, insets). Because the ER is continuous, we also used repetitive photobleaching of a small region to deplete signal from the entire ER network.

Following bleaching, these ER markers were not detected in starvation-induced autophagosomes, suggesting no transfer of ER markers to autophagosomes had taken place. (Figure S2).

Only the YFP-Mito^{cb5}TM mitochondrial outer membrane marker showed extensive overlap with autophagosomes. YFP-Mito^{cb5}TM was present on nearly 80% of CFP-LC3 positive autophagosomes after a 2 hr starvation (Figures 3A and 3B).

Notably, this observation was specific to starvation-induced autophagy. YFP-Mito^{cb5}TM did not colocalize with autophagosomes formed in response to ER stress and calcium perturbation (Figure S3). YFP-Mito^{cb5}TM stably associated with autophagic membranes. Photobleaching YFP-Mito^{cb5}TM signal was used to deplete all signal except that present on isolated autophagic vesicles. YFP-Mito^{cb5}TM showed persistent signal on these isolated autophagosomes for > 3 min (Figure 3C).

Autophagosome/Mitochondria Overlap during Starvation Is Not Due to Mitophagy

We next asked whether overlap of YFP-Mito^{cb5}TM mitochondrial outer membrane marker with the autophagic marker was due to induction of mitophagy, a process wherein mitochondria are captured and degraded (Mijaljica et al., 2007). This predicts more overlap of matrix and inner membrane mitochondrial markers with CFP-LC3 positive structures compared to an outer mitochondrial marker. We thus evaluated co-localization of mitochondrial matrix and inner membrane markers with CFP-LC3 after autophagic induction. Mitochondrial matrix was labeled with yellow fluorescent protein fused to the targeting sequence of cytochrome c oxidase subunit VIII. Inner membrane was labeled with 10N-nonyl acridine orange (a dye that binds
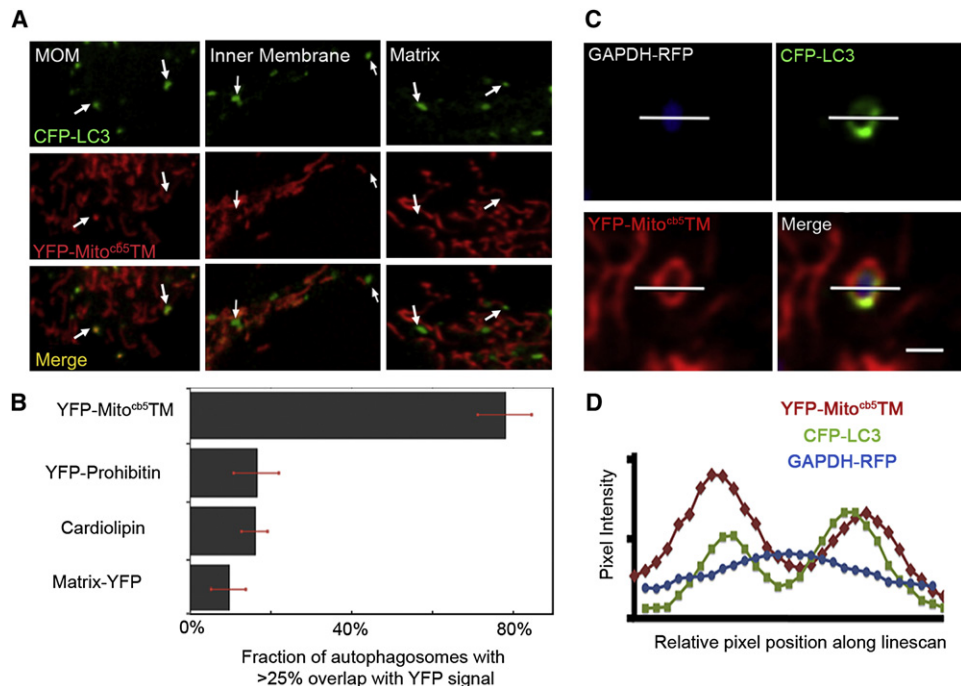
Figure 4. Assessing Whether Mitophagy Underlies YFP-Mito^{cb5}TM Signal on Autophagosomes

(A) CFP-LC3 signal overlap with mitochondrial outer membrane (MOM), inner membrane and matrix markers. MOM, inner membrane, and matrix markers revealed robust overlap for the outer membrane, but not inner membrane and matrix (see arrows).

(B) Quantification of CFP-LC3 signal overlap with mitochondrial markers (as described in Figure 3B).

(C) Association of YFP-Mito^{cb5}TM with autophagosomal membrane. NRK58B cells were transfected with YFP-Mito^{cb5}TM and GAPDH-RFP and starved. Freely diffusing cytosolic GAPDH-RFP signal was depleted by photobleaching to reveal CFP-LC3/YFP-Mito^{cb5}TM/GAPDH-RFP positive autophagosomes. Images of these structures revealed YFP-Mito^{cb5}TM present on the membrane, not trapped in the lumen. The scale bar represents 1.5 μm.

(D) Line-scan evaluation of CFP-LC3/YFP-Mito^{cb5}TM/GAPDH-RFP signal in autophagosomes. CFP-LC3 and YFP-Mito^{cb5}TM pixel values along a transecting line (shown in [C]) exhibited two delineated peaks (membrane). GAPDH-RFP pixel values along this line exhibited a bell-curve like signal profile (lumen). (See also Figure S4.)

cardiolipin in the inner mitochondrial membrane (Petit et al., 1992). Neither marker showed a comparable degree of overlap with the autophagosomal marker after starvation (Figures 4A and 4B). Similarly, the inner membrane marker Prohibitin-YFP showed dramatically less autophagosome-associated signal (Figure 4B). Contrary to what mitophagy predicts, matrix and inner mitochondrial markers did not overlap with CFP-LC3-positive structures induced by starvation.

Mitophagy also predicts mitochondrial components should be captured inside autophagosomes. To test this, we examined autophagosomes in cells expressing YFP-Mito^{cb5}TM and GAPDH-RFP. High-resolution imaging resolved isolation membranes of autophagosomes around sequestered GAPDH-RFP signal (Figure 4C). Line profiles of GAPDH-RFP within autophagosomes exhibited single bell-shaped intensity profiles, consistent with soluble protein trapped in the lumen of the autophagosomes. By contrast, YFP-Mito^{cb5}TM showed well-delineated intensity peaks at the limiting membranes of autophagic vesicles (Figure 4D). This indicated that YFP-Mito^{cb5}TM in autophagosomes was present on limiting membranes of autophagosomes, and that the autophagosome lumens contained cytosolic components, not mitochondria.

Finally, we compared starvation with conditions known to induce mitophagy. Mitophagy can be induced by staurosporine/ Z-VAD-FMK treatment to simultaneously damage mitochondria and inhibit pan-caspase activity (Colell et al., 2007). In these conditions, flow cytometry revealed loss of mitochondrial mass in a significant fraction of treated cells. Additionally, we observed autophagosomes in treated NRK58B cells that captured both mitochondrial matrix and inner membrane. Starvation, in contrast, produced neither appreciable loss of mitochondrial mass nor apparent capture of entire mitochondria (Figure 4; Figure S4). We concluded that mitophagy does not underlie the presence of YFP-Mito^{cb5}TM in autophagosomal membranes during starvation in our system.

Starvation-Induced Autophagosomes Emerge from Sites on Mitochondria

We next considered other scenarios that could result in overlap of the mitochondrial outer membrane marker with the autophagosome marker. One possibility is that mitochondrial outer membrane is used in autophagosome biogenesis. We asked if we could visualize outgrowth of autophagosomes from mitochondria. Starved NRK cells expressing GFP-LC3 and
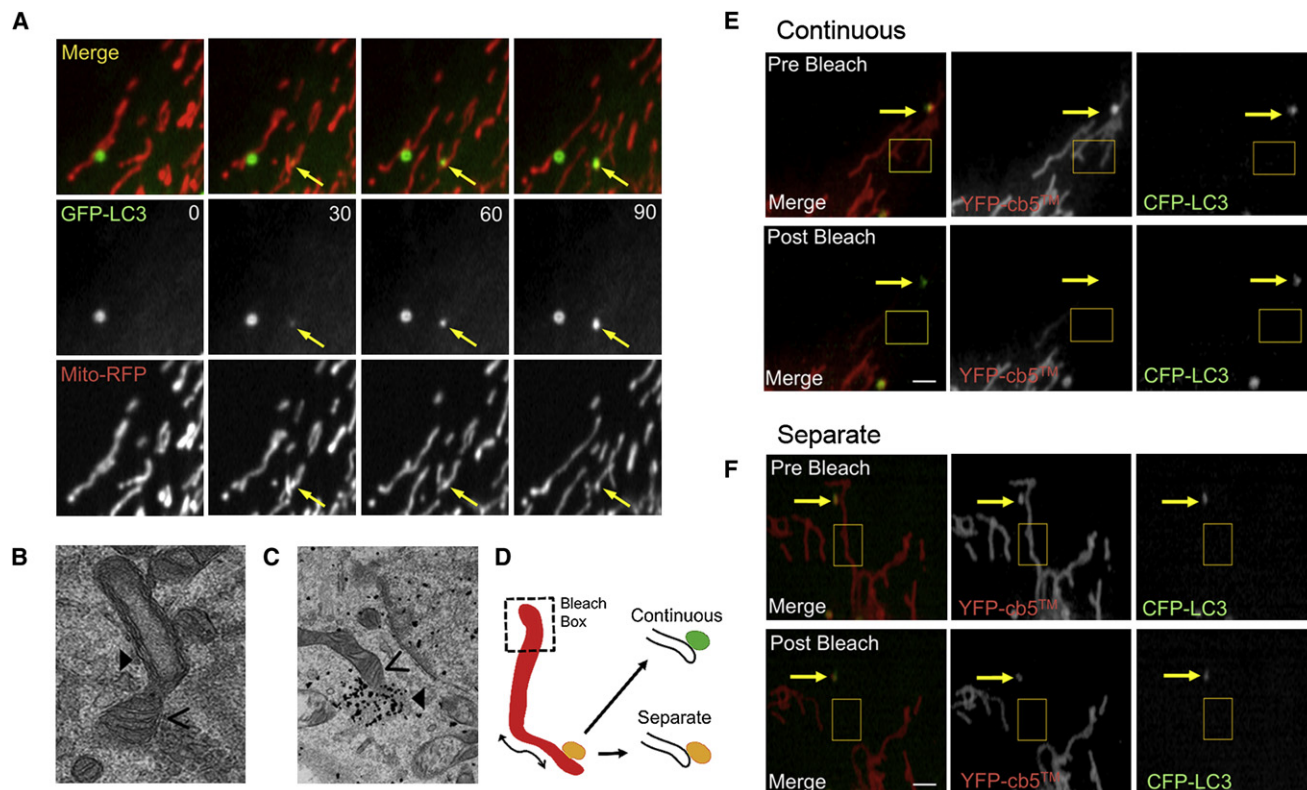
Figure 5. Assessing Association of Starvation-Induced Autophagosomes and Mitochondria

(A) Live-cell imaging of autophagosomes and associated mitochondrial elements. Live NRK cells transfected with mitochondria matrix (Mito-RFP) and autophagosome marker (GFP-LC3) were imaged following starvation. Autophagosomes grew during tight association with mitochondrial elements. (See also Movie S4.)

(B) Electron microscopy of starved cells. Electron micrographs revealed multilammelar structures (closed arrowhead) tightly associated with mitochondrial elements (open arrowhead) that excluded mitochondrial matrix.

(C) Immuno EM of starved NRK58B cells labeled with gold-conjugated antibodies against CFP revealed clusters of gold particles (closed arrowhead) tightly associated with proximal mitochondrial elements (open arrowhead).

(D) Schematic of assay to assess autophagosome/mitochondria membrane association. Photobleaching distal end of a mitochondrial element depletes YFP-Mito^{cb5}TM signal diffusing throughout the membrane. If YFP-Mito^{cb5}TM positive autophagosomes share membranes with mitochondria, all YFP-Mito^{cb5}TM signal will be depleted via diffusion between the associated organelles. YFP-Mito^{cb5}TM positive autophagosomes that are near but not continuous with the MOM will retain YFP-Mito^{cb5}TM signal.

(E) Results of assay described in D. Autophagosomes that appeared along mitochondrial elements were identified. Distal ends of associated mitochondrial elements were targeted with 405 nm and 490 nm light (yellow box). Here, distal photobleaching depleted signal both from the mitochondrion and associated autophagosome outside the bleached region (see loss of signal, bottom row, middle panel). The scale bar represents 2 μm.

(F) Autophagosomes that were spatially close but not associated retained signal after photobleaching of proximal mitochondrial elements (see retention of signal, bottom row, middle panel). The scale bar represents 2 μm. (See also Figure S5 and Movie S5.)

Mito-RFP revealed GFP-LC3 punctae that first formed in association with mitochondria and retained that association despite highly dynamic mitochondrial movements (Figure 5A; Movie S4). Another autophagosome marker GFP-Atg5 showed similar behavior. Membrane association of the Atg5/Atg12/Atg16 complex is a prerequisite for LC3 recruitment to membranes (Mizushima et al., 2001). In starved NRK cells, GFP-Atg5 punctae first appeared along mitochondrial elements and persisted along these elements through their lifetime (Figure S5; Movie S5).

Transmission EM further supported mitochondrial membrane involvement in autophagosome formation. Micrographs of starved NRK58B and wild-type NRK cells revealed multilamellar autophagosomal structures that were never observed in unstarved cells. Most of these structures were isolated organelles; however some were closely apposed to or continuous with mitochondrial elements (Figure 5B). These structures excluded mitochondria inner membrane and matrix and showed luminal electron density like that of the cytoplasm. Dimensions of the structures correlated well with dimensions of CFP-LC3 positive structures observed by confocal microscopy. To address whether the structures were CFP-LC3-positive, starved NRK58B cells were fixed, permeabilized and labeled with gold conjugated antibodies to CFP (Figure 5C). Clusters of gold label were observed in structures adjacent to mitochondria.

Membrane Continuity between Outer Mitochondrial Membrane and Newly Formed Autophagosomes

The above results suggested starvation-induced autophagosomes emerge from mitochondrial outer membranes. If so, mitochondria and autophagosomes should share membranes early
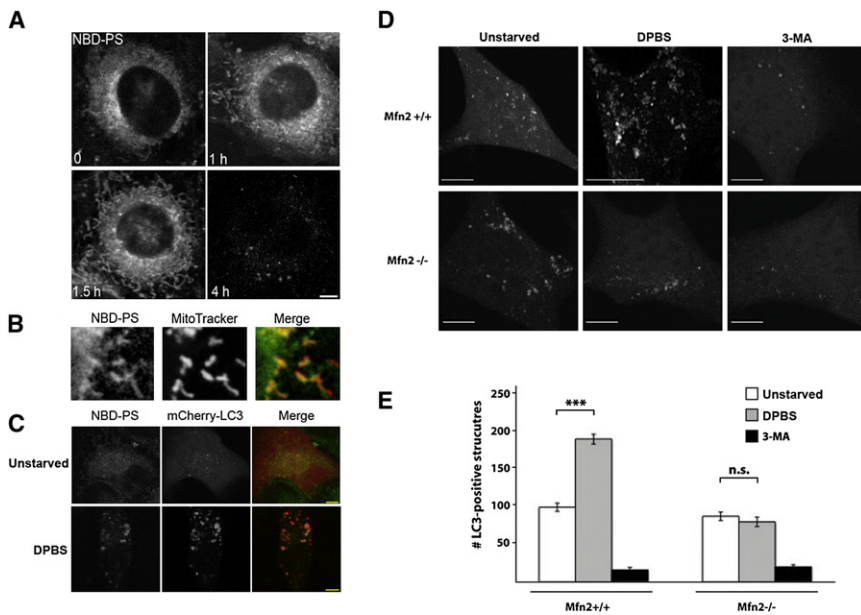
Figure 6. Mitochondrial Lipid Utilization in Autophagosome Formation

(A) Time course following loading exogenous NBD-phosphatidylserine (NBD-PS). NRK cells were exposed to NBD-PS, washed, and maintained in complete media. NBD-PS signal rapidly accumulated in mitochondria and was subsequently lost. The scale bar represents 5 μm.

(B) Mitotracker red and NBD-PS labeling confirmed accumulation of NBD-PS signal in mitochondria 1 hr after NBD-PS loading.

(C) NBD-labeling of starvation-induced autophagosomes. NBD-PS was allowed to accumulate in mitochondria for 1 hr prior to starvation. Upon starvation, NBD-signal accumulated in mCherry-LC3 positive autophagosomes. The scale bar represents 5 μm.

(D) Disrupting ER-mitochondria connections by Mitofusin 2 deficiency. Mfn2$^{+/+}$ and Mfn2$^{-/-}$ MEF cells were transfected with mCherry-LC3. Mfn2$^{+/+}$ and Mfn2$^{-/-}$ cells under nutrient-rich conditions showed comparable basal autophagy. Following starvation, Mfn2$^{+/+}$ cells showed a dramatic increase in number of autophagic structures and depletion of the cytoplasmic pools of mCherry-LC3. In contrast, Mfn2$^{-/-}$ cells (like 3-MA treated cells) failed to induce autophagosomes.

(E) Quantification of mCherry-LC3 positive structures in Mfn2$^{+/+}$ and Mfn2$^{-/-}$ cells, counted in 25 cells in three independent experiments.

in autophagosome formation. We often observed small CFP-LC3/YFP-Mito^{cb5}TM positive structures present along YFP-Mito^{cb5}TM-labeled tubular mitochondria. High-resolution images could not reveal whether YFP-Mito^{cb5}TM positive-autophagosomes were in close proximity with mitochondria or whether they actually shared membrane. We used targeted laser photobleaching to discriminate between these possibilities. Mitochondrial elements with associated autophagic structures were identified. Small regions at the distal ends of mitochondrial elements were photobleached with 405 nm and 489 nm laser lines. We predicted membrane continuity would allow YFP signal from both mitochondria and associated autophagosomes to be depleted; without continuity, only mitochondrial YFP signal would be depleted (schematic in Figure 5D). Repetitive photobleaching rapidly depleted YFP-Mito^{cb5}TM signal along the entire length of targeted mitochondrial elements due to rapid diffusion of YFP-Mito^{cb5}TM into the distal photobleached regions. In some instances, diffusion of YFP -Mito^{cb5}TM into the bleached region also depleted signal that overlapped with CFP-LC3 signal (Figure 5E). Direct post-translational insertion of YFP-Mito^{cb5}TM into autophagosome membranes and close spatial proximity to mitochondria cannot account for these results. The lateral exchange of YFP-Mito^{cb5}TM between mitochondrial elements and regions of CFP-LC3 overlap instead indicates membrane continuity exists between maturing autophagosomes and associated mitochondria. The majority of autophagosomes did not exhibit this behavior, and it was not observed with large (>800nm) CFP-LC3/YFP-Mito^{cb5}TM positive structures (Figure 5F). These findings suggested that continuity of autophagosome and mitochondria membranes is transient,

likely representing an early event in formation of starvation-induced autophagosomes.

Lipid Delivery from Mitochondria to Newly Forming Autophagosomes

If mitochondrial outer membranes are a membrane source for autophagosome formation, lipid components of mitochondrial outer membranes should be found in autophagosomal membranes. No known lipid markers uniquely label the outer mitochondrial membrane. However, we took advantage of the well-established transfer of lipids from ER to mitochondria. Phosphotidylserine (PS) is readily transferred from ER to mitochondria where it is converted to phosphotidylethanolamine (PE) by the mitochondrial enzyme phosphotidylserine decarboxylase (Vance and Vance, 2004). To test if lipid is transferred between mitochondrial and autophagosomal membranes, we loaded cells with 18:1-06:0 N-[7-Nitrobenz-2-oxa-1,3-diazol-4-yl] phosphotidylserine (NBD-PS), a fluorescent analog of PS that has been used to label mitochondria (Kobayashi and Arakawa, 1991). We observed fluorescent signal from NBD-PS first in ER membranes and subsequently in mitochondrial membranes (Figures 6A and 6B). When cells exhibiting mitochondrial labeling were starved, NBD fluorescence appeared in induced autophagosomes (Figure 6C). Signal in autophagosomes was increased by drug treatments that disrupt fusion of autophagosomes with lysosomes (data not shown). The NBD lipid probe thus transfers from mitochondria to autophagosomes, consistent with the behavior of the protein marker YFP-Mito^{cb5}TM, further supporting a role for mitochondrial membranes in autophagosome formation.
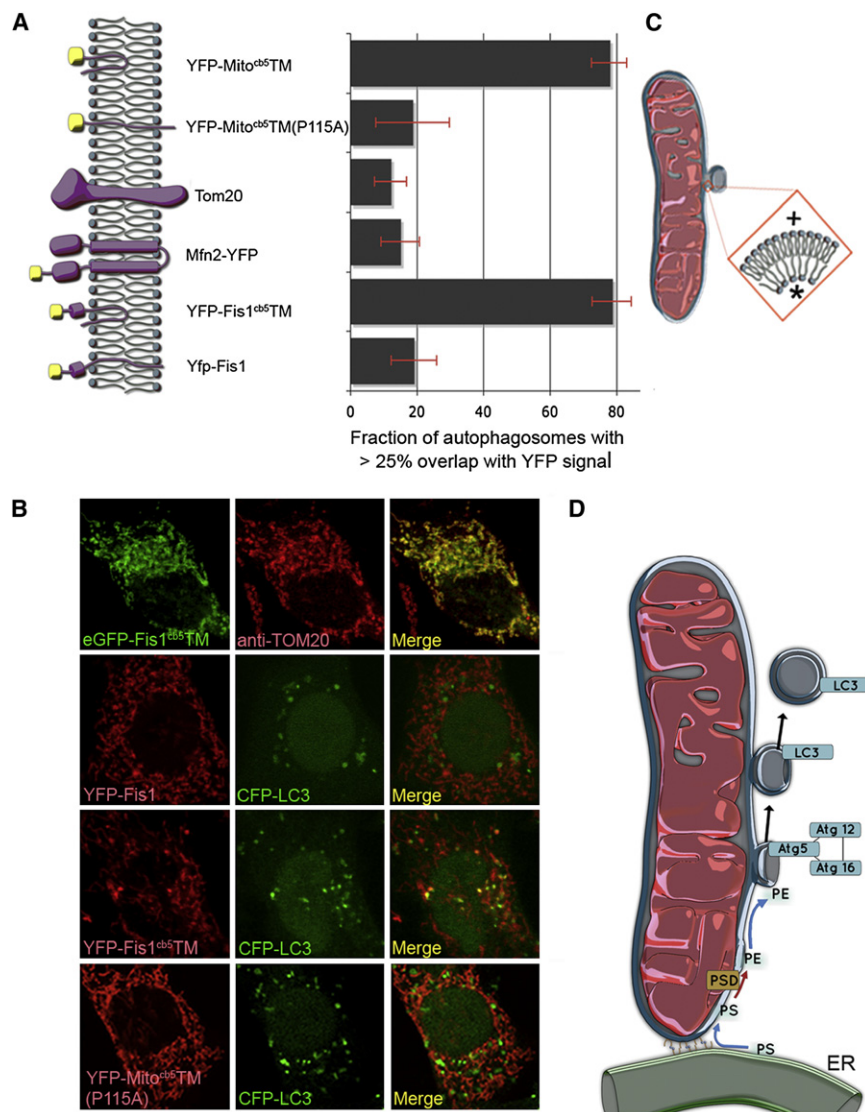
Figure 7. Maintenance of Mitochondria during Autophagosome Biogenesis

(A) Transmembrane domains (TMDs) that span both lipid bilayer leaflets are excluded from autophagosomes. YFP-Mito^{cb5}TM can interact with only the outer leaflet. Other outer membrane mitochondrial proteins with TMDs that span both leaflets fail to label autophagosomes. Consistent with this, replacement of the Fis1 TMD with the Mito-cb5 tail (YFP-Fis1^{cb5}TM) permits its delivery to autophagosomes. Forcing the TMD of YFP-Mito-cb5 into a form that spans both leaflets (YFP-Mito^{cb5}TM(P115A))–abolishes its delivery to autophagosomes.

(B) Fis1^{cb5}TM targeting to mitochondria in unstarved cells, delivery to autophagosomes, and effect of the P115A mutation.

(C) Schematic of proposed autophagosome bud site. Sharp membrane curvature promotes different lipid compositions on the inner and outer leaflets.

(D). Schematic for a proposed means by which starvation-induced autophagosomes utilize mitochondrial membrane during biogenesis (described in Discussion).

Mitochondrial Proteins Are Largely Excluded from Autophagosomes

Close contacts of mitochondria with ER could resupply lipid to mitochondria to compensate for lipid transfer into autophagosomes. But what prevents mitochondrial proteins from being depleted during starvation? To address this, we examined whether protein transfer from the outer mitochondrial membrane to autophagosomes was selective. We found this to be the case. Unlike YFP-Mito^{cb5}TM, other outer mitochondrial membrane proteins we examined (e.g., Tom20, Mfn2, and Fis1) showed no transfer into starvation-induced autophagosomes (Figure 7A). Thus, key mitochondrial outer membrane proteins are excluded from autophagosomes.

How might most mitochondrial membrane proteins be excluded from autophagosomes? Sharp membrane curvature can impose selective protein transfer via steric and topological constraints (Schmidt and Nichols, 2004). We speculated that a selective barrier at an autophagosomal budding site could prevent mitochondrial membrane proteins from entering autophagosomes (Figure 7C). Previous studies of ER cb5 identified a proline in the transmembrane domain that permits formation of a kinked helix that intercalates into only the outer leaflet of the targeted bilayer (Figure 7A) (Takagaki et al., 1983; Vergeres and Waskell, 1995). To evaluate if transfer from mitochondria to autophagosomes requires an outer leaflet interaction, we mutated the proline in the cb5 transmembrane domain of YFP-Mito^{cb5}TM. This proline to alanine mutation forces the TMD of the ER isoform into a helical coil that spans both leaflets (Vergeres and Waskell, 1995). Mutant YFP-Mito^{cb5}TM(P115A)

Cells Lacking Mitofusin 2 Do Not Form Autophagosomes in Response to Starvation

As further evidence for mitochondrial membrane involvement in autophagy, we pursued the observation that mitochondrial lipid (which had originated in the ER) is transferred to autophagosomes in starved cells. We reasoned that if this is crucial for making autophagosomes, perturbing ER/mitochondria contacts to impede lipid transfer might inhibit starvation-induced autophagy. We used a cell line lacking mitofusin 2 (Mfn2), a mitochondrial fusion factor shown to help tether mitochondria to ER (de Brito and Scorrano, 2008). YFP-LC3 was transiently transfected into the Mfn2$^{-/-}$ cells and control cells. The cells were starved for 2 hr and examined by confocal microscopy. Whereas robust autophagic induction occurred in control cells, no induction occurred in cells lacking Mfn2 (Figures 6D and 6E). Mfn2 tethering activity is therefore necessary for autophagosome formation during starvation, supporting the idea that membrane lipids of autophagosomes (which are PE enriched) derive from mitochondria in starved cells.

efficiently targeted mitochondria. However, it did not label auto-phagosomes; the degree of co-localization was equivalent to that observed for mitochondrial matrix (see Figure 4C) and non-cb5 outer mitochondrial membrane markers (Figures 7A and 7B). The exclusion of YFP-Mito^{cb5}TM(P115A) from autopha-gosomes supports our proposal that a diffusion barrier exists during autophagosome formation, and only proteins associating with the outer leaflet of the outer mitochondrial membrane can traverse this barrier. This could underlie the paucity of integral membrane proteins observed in autophagosomal membranes (Fengsrud et al., 2000), and closely apposed membranes of autophagic vesicles could exclude proteins in the inner-mem-brane space.

To further test this idea, we asked whether the transmembrane domain of YFP-Mito^{cb5}TM might permit transfer of other mito-chondrial membrane proteins to autophagosomes. Fis1 inter-acts with dynamin-like protein DLP1 at the outer membrane to promote mitochondrial fission. YFP-Fis1 labels mitochondria but not autophagosomes (Figures 7A and 7B). Replacement of the Fis1 TMD with the Mito-cb5 tail (YFP-Fis1^{cb5}TM) is sufficient to permit transfer of the protein to autophagosomes. The Mito-cb5 tail therefore may be a unique type of lipid anchor that allows transfer of proteins from mitochondria to autophagosomes.

DISCUSSION

A growing body of research supports a connection between mitochondria and autophagosomes. Key autophagy proteins including Beclin-1, yeast Atg9p and Atg5 can localize to mito-chondria (Reggiori et al., 2005; Takahashi et al., 2007b; Yousefi et al., 2006), and several mitochondrial proteins (e.g., smARF, Bif-1/EndophillinB, Sirt1) positively regulate autophagy (Lee et al., 2008; Reef et al., 2006; Takahashi et al., 2007a). Knock-down of Bif-1 and Sirt1 suppress induction of autophagy during starvation. Reports of interplay between autophagy and mito-chondria are often ascribed to mitophagy. Our data suggest an alternative—that mitochondria can participate in formation of autophagosomes.

Here, we show autophagosome inception occurs along mito-chondria. *Atg5* and LC3 transiently localize to punctae on mito-chondria. We found that the tail-anchor of a mitochondrial outer membrane protein also labels autophagosome membranes and that this tail anchor is sufficient to deliver another outer mitochon-drial membrane protein to autophagosomes. We demonstrate that this marker can be depleted from autophagosomes by pho-tobleaching associated mitochondrial elements, indicating mito-chondria and autophagosomes transiently share membranes. Tomography and immuno-EM reveal autophagic structures associated with mitochondria. We provide evidence that a diffu-sion barrier prevents delivery of mitochondrial proteins, but not mitochondrial lipids, to autophagosomes. Consistent with a requirement for mitochondrial lipids, we show autophagosome induction during starvation is severely inhibited when ER/mito-chondrial connections are impaired in cells lacking Mfn2.

One plausible scenario by which autophagosomes could form involves imposing membrane curvature and subsequent fusion at the outer mitochondrial membrane (Figure 7D). The Vps34/Beclin-1 complex may mark an initiation site. Phosphorylation

of phosphoinositides and Bif-1 BAR domain interactions with membrane could create and stabilize a microdomain that recruits the Atg5/Atg12/Atg16 complex. Oligomerization of this complex, reported in (Kuma et al., 2002; Mizushima et al., 2003), could then form a coat and expand the initiation site. LC3 conjugation to PE at the site could stabilize local concentra-tions of PE in the outer leaflet, and support continued outgrowth. Notably, PE can impose a negative radius of curvature to generate a cup-like structure (Thomas and Poznansky, 1989; van Meer et al., 2008). Fusion of distal edges could then form a multi-lamellar structure. LC3 can catalyze homotypic membrane fusion in an in vitro system (Nakatogawa et al., 2007). This scenario is consistent with activities of core autophagy machinery, and would allow for specific lipid enrichment and outgrowth from an existing membrane.

Given autophagy machinery can target a membrane and promote membrane curvature, autophagosomes could form from different sources. Core autophagy machinery is reported to target membranes of different origins. While ER stress-induced autophagosomes can utilize ER membrane (Bernales et al., 2006), LC3 can also be recruited to membranes derived from the plasma membrane (Sanjuan et al., 2007). We found that NRK58B cells treated with thapsigargin (Brostrom and Brostrom, 2003; Tadini-Buoninsegni et al., 2008) form CFP-LC3 positive struc-tures, consistent with other reports of ER stress induced autoph-agy (Ogata et al., 2006; Sakaki et al., 2008). However, the struc-tures do not label with YFP-Mito^{cb5}TM (**Supp Figure S3**). Utilization of different membranes in autophagosome biogenesis may produce different classes of autophagosomes with behav-iors specific to induction conditions (**Supp Figure S6**). What membrane is utilized during autophagy therefore may collapse to a question of how autophagosome assembly is initiated at diverse sites.

Why might starvation specifically utilize mitochondrial mem-brane? A little-explored aspect of autophagy is its role in fluxing lipids through otherwise disconnected compartments. Our pho-tochase data indicates that a significant amount of membrane is moving from autophagosomes to lysosomes via fusion of membranes of these organelles. The lipid target of LC3, PE, is an abundant lipid transferred by autophagosomes. PE is synthe-sized principally at two sites—in the ER via the CDP-ethanolamine pathway, and in mitochondria via decarboxylation of PS (Vance, 2008). PE synthesis in the ER utilizes DAG and exogenous ethanolamine. PE synthesis in mitochondria utilizes phosphoti-dylserine from the ER. Under starvation conditions, sources for exogenous ethanolamine and DAG (produced following growth factor engagement) are restricted and may limit PE synthesis in the ER. Autophagy may counter this by routing mitochondrial-derived PE to lysosomes, and subsequently via retrograde trans-port, back through the secretory pathway. Mitochondria lipid contribution to autophagosomal membranes may therefore contribute to lipid homeostasis, in addition to nutrient recycling.

Given a significant flux of lipid, one prediction of utilizing mito-chondrial lipids is depletion of mitochondria. However, starva-tion-induced autophagy does not cause loss of mitochondrial mass in our system. Other conditions reported to induce autoph-agy (e.g., Sirt1 overexpression) show concurrent autophago-some proliferation and increased mitochondrial mass (Lee

et al., 2008). How might mitochondrial mass be maintained? A major source for mitochondrial phospholipids is the ER. Mitochondrial-associated membranes act as bridges between mitochondria and ER in both yeast and mammals, where PS and other phospholipids are transferred to mitochondria (Achleitner et al., 1999; Bozidis et al., 2008). An unexplored question is whether autophagy promotes transfer of lipid from the ER to mitochondria. We have evaluated whether ER/mitochondrial connections are important for autophagic induction. Loss of Mfn2 disrupts connections between the ER network and mitochondria (de Brito and Scorrano, 2008). We found that Mfn2 knockout cells fail to produce autophagosomes when starved. Therefore, lipid contribution from the ER to mitochondria appears to be critical for starvation-induced autophagy.

This ER/mitochondrial connection may underlie recent findings implicating ER membrane in autophagosome formation. During starvation, DFCP1, a phospholipid binding protein in the ER, translocates to sites of autophagosome formation (Axe et al., 2008). Atg5 and LC3 markers surround DFCP1, and the authors present a model in which autophagosomes form from ER membrane. Our data suggest another possibility—that DFCP1 sites may be sites of connection between the ER and mitochondria that respond to starvation. Rapid formation of autophagosomes may drive lipid transfer from the ER to mitochondria where lipids are modified and utilized in autophagosome biogenesis.

Whether autophagosomes form de novo or from pre-existing membranes is a long-standing debate. Investigating how autophagosome assembly is initiated and proceeds remains difficult (Juhasz and Neufeld, 2006). The findings presented here indicate that mitochondria participate directly in formation of autophagosomes. Utilization of the outer membrane of mitochondria defines a new intracellular pathway from mitochondria to the autophagosomal/lysosomal system. Budding of vesicles from mitochondria that transit to peroxisomes has been reported (Neuspiel et al., 2008). Such events, together with the mitochondrial pathway to autophagosomes reported here, may underlie the constitutive movement of mitochondrial-derived factors–e.g., heme (Rajagopal et al., 2008)–to different cellular locations, and implicate mitochondrial involvement in as yet unappreciated aspects of cell biology.

EXPERIMENTAL PROCEDURES

Plasmid Constructs
Plasmid information and constructions are outlined in the Supplemental Information.

Cell Culture
Cells were maintained in DMEM/10%FBS/Penn/Strep. Clonal cell lines were selected with 800ug/mL G418. All live cell imaging was performed on cells grown in LabTek chambers (Nalge Nunc International, Naperville, IL) and maintained either in CO2 independent media (Invitrogen, Carlsbad, CA) or appropriate media formulations at the scope. Transient transfections were done 16 hr prior to imaging with Fugene 6 transfection reagent (Roche, Indianapolis, IN).

Media Treatments
Starvation was induced by 2–4 hr incubation in DPBS with D-glucose and sodium pyruvate (Invitrogen SKU# 14287-080), or, where noted, serum-free DMEM or HBSS.

Fluorescence Microscopy
Images were aquired on Zeiss LSM 510 Meta, Zeiss LSM DUO, and Perkin Elmer UltraView ERS 6FO-US systems (see Supplemental Information). Images were analyzed with LSM (Carl Zeiss MicroImaging, Inc.) and ImageJ (NIH/public domain) software. Brightness and contrast were adjusted in Photoshop CS (Adobe). For time-lapse sequences, identical adjustments were applied to all frames using Photoshop batch function and reassembled into movie files with QuickTime Pro.

Live-Cell Staining
LysoTracker DND99 and Mitotracker RedCMXRos (Invitrogen Molecule Probes) were added directly to media at 100 nM and 150 nM respectively, incubated for 10 min, and washed immediately before imaging. NBD-PS was reconstituted to a 2.2 mM stock in sterile PBS and loaded at 0.22 mM final concentration for 30 min. See Supplemental Information for lipid formulation.

Pharmaceutical Treatments
3-methyladenine (Sigma, M9281) was used at 10 mM. Thapsigargin (Sigma, T9033) was used at 25 nM. Digitonin (Calbiochem, 300410) was used at 1:1000 of a 6% stock. KHM buffer is described in (Lorenz et al., 2006). Chloroquine (Sigma, C6628) was used at 1:100 of a 100 μM stock. See Supplemental Information for additional details.

Electron Microscopy
Cells were fixed with 2.5% glutaraldehyde in 0.1 M Cacodylate buffer, and post-fixed in reduced osmium prior to Epon embedding. 70–100 nm sections were stained with lead citrate and imaged with a Tecnai 20 TEM (FEI Company, Netherlands) at 120 kV. For ImmunoEM, cells were fixed in 4% paraformaldehyde, blocked with 1% bovine serum albumin in PBS. Permeabilized cells (0.05% saponin in PBS / BSA 1%) were incubated with primary GFP antibody (rabbit anti-GFP; Molecular Probes) and subsequently incubated with nano-gold-conjugated secondary antibodies (Nanoprobes). Cells were fixed with glutaraldehyde, treated with gold enhancement mixture for 6 min and post-fixed in reduced osmium prior to embedding in Epon. 70–100 nm sections were cut and stained with lead citrate prior to imaging.

SUPPLEMENTAL INFORMATION

Supplemental Information includes Extended Experimental Procedures, six figures, and five movies and can be found with this article online at doi:10.1016/j.cell.2010.04.009.

REFERENCES

Achleitner, G., Gaigg, B., Krasser, A., Kainersdorfer, E., Kohlwein, S.D., Perktold, A., Zellnig, G., and Daum, G. (1999). Association between the endoplasmic reticulum and mitochondria of yeast facilitates interorganelle transport of phospholipids through membrane contact. Eur. J. Biochem. 264, 545–553.

Axe, E.L., Walker, S.A., Manifava, M., Chandra, P., Roderick, H.L., Habermann, A., Griffiths, G., and Ktistakis, N.T. (2008). Autophagosome formation from membrane compartments enriched in phosphatidylinositol 3-phosphate and dynamically connected to the endoplasmic reticulum. J. Cell Biol. 182, 685–701.

Bernales, S., McDonald, K.L., and Walter, P. (2006). Autophagy counterbalances endoplasmic reticulum expansion during the unfolded protein response. PLoS Biol. *4*, e423.

Bjorkoy, G., Lamark, T., Brech, A., Outzen, H., Perander, M., Overvatn, A., Stenmark, H., and Johansen, T. (2005). p62/SQSTM1 forms protein aggregates degraded by autophagy and has a protective effect on huntingtin-induced cell death. J. Cell Biol. *171*, 603–614.

Borgese, N., Gazzoni, I., Barberi, M., Colombo, S., and Pedrazzini, E. (2001). Targeting of a tail-anchored protein to endoplasmic reticulum and mitochondrial outer membrane by independent but competing pathways. Mol. Biol. Cell *12*, 2482–2496.

Bozidis, P., Williamson, C.D., and Colberg-Poley, A.M. (2008). Mitochondrial and secretory human cytomegalovirus UL37 proteins traffic into mitochondrion-associated membranes of human cells. J. Virol. *82*, 2715–2726.

Brostrom, M.A., and Brostrom, C.O. (2003). Calcium dynamics and endoplasmic reticular function in the regulation of protein synthesis: implications for cell growth and adaptability. Cell Calcium *34*, 345–363.

Colell, A., Ricci, J.E., Tait, S., Milasta, S., Maurer, U., Bouchier-Hayes, L., Fitzgerald, P., Guio-Carrion, A., Waterhouse, N.J., Li, C.W., et al. (2007). GAPDH and autophagy preserve survival after apoptotic cytochrome c release in the absence of caspase activation. Cell *129*, 983–997.

D'Arrigo, A., Manera, E., Longhi, R., and Borgese, N. (1993). The specific subcellular localization of two isoforms of cytochrome b5 suggests novel targeting pathways. J. Biol. Chem. *268*, 2802–2808.

de Brito, O.M., and Scorrano, L. (2008). Mitofusin 2 tethers endoplasmic reticulum to mitochondria. Nature *456*, 605–610.

Doelling, J.H., Walker, J.M., Friedman, E.M., Thompson, A.R., and Vierstra, R.D. (2002). The APG8/12-activating enzyme APG7 is required for proper nutrient recycling and senescence in Arabidopsis thaliana. J. Biol. Chem. *277*, 33105–33114.

Fengsrud, M., Erichsen, E.S., Berg, T.O., Raiborg, C., and Seglen, P.O. (2000). Ultrastructural characterization of the delimiting membranes of isolated autophagosomes and amphisomes by freeze-fracture electron microscopy. Eur. J. Cell Biol. *79*, 871–882.

Furuya, N., Yu, J., Byfield, M., Pattingre, S., and Levine, B. (2005). The evolutionarily conserved domain of Beclin 1 is required for Vps34 binding, autophagy and tumor suppressor function. Autophagy *1*, 46–52.

Hailey, D.W., and Lippincott-Schwartz, J. (2009). Using photoactivatable proteins to monitor autophagysome lifetime. Methods Enzymol. *452*, 25–45.

Hayashi-Nishino, M., Fujita, N., Noda, T., Yamaguchi, A., Toshimori, T., and Yamamoto, A. (2009). A subdomain of the endoplasmic reticulum forms a cradle for autophagosome formation. Nat. Cell Biol. *12*, 1433–1437.

Hoyvik, H., Gordon, P.B., Berg, T.O., Stromhaug, P.E., and Seglen, P.O. (1991). Inhibition of autophagic-lysosomal delivery and autophagic lactolysis by asparagine. J. Cell Biol. *113*, 1305–1312.

Juhasz, G., and Neufeld, T.P. (2006). Autophagy: a forty-year search for a missing membrane source. PLoS Biol. *4*, e36.

Kabeya, Y., Mizushima, N., Ueno, T., Yamamoto, A., Kirisako, T., Noda, T., Kominami, E., Ohsumi, Y., and Yoshimori, T. (2000). LC3, a mammalian homologue of yeast Apg8p, is localized in autophagosome membranes after processing. EMBO J. *19*, 5720–5728.

Kobayashi, T., and Arakawa, Y. (1991). Transport of exogenous fluorescent phosphatidylserine analogue to the Golgi apparatus in cultured fibroblasts. J. Cell Biol. *113*, 235–244.

Kuma, A., Hatano, M., Matsui, M., Yamamoto, A., Nakaya, H., Yoshimori, T., Ohsumi, Y., Tokuhisa, T., and Mizushima, N. (2004). The role of autophagy during the early neonatal starvation period. Nature *432*, 1032–1036.

Kuma, A., Mizushima, N., Ishihara, N., and Ohsumi, Y. (2002). Formation of the approximately 350-kDa Apg12-Apg5.Apg16 multimeric complex, mediated by Apg16 oligomerization, is essential for autophagy in yeast. J. Biol. Chem. *277*, 18619–18625.

Lederer, F., Ghrir, R., Guiard, B., Cortial, S., and Ito, A. (1983). Two homologous cytochromes b5 in a single cell. Eur. J. Biochem. *132*, 95–102.

Lee, I.H., Cao, L., Mostoslavsky, R., Lombard, D.B., Liu, J., Bruns, N.E., Tsokos, M., Alt, F.W., and Finkel, T. (2008). A role for the NAD-dependent deacetylase Sirt1 in the regulation of autophagy. Proc. Natl. Acad. Sci. USA *105*, 3374–3379.

Lorenz, H., Hailey, D.W., and Lippincott-Schwartz, J. (2006). Fluorescence protease protection of GFP chimeras to reveal protein topology and subcellular localization. Nat. Methods *3*, 205–210.

Mijaljica, D., Prescott, M., and Devenish, R.J. (2007). Different fates of mitochondria: alternative ways for degradation? Autophagy *3*, 4–9.

Mizushima, N., Kuma, A., Kobayashi, Y., Yamamoto, A., Matsubae, M., Takao, T., Natsume, T., Ohsumi, Y., and Yoshimori, T. (2003). Mouse Apg16L, a novel WD-repeat protein, targets to the autophagic isolation membrane with the Apg12-Apg5 conjugate. J. Cell Sci. *116*, 1679–1688.

Mizushima, N., Yamamoto, A., Hatano, M., Kobayashi, Y., Kabeya, Y., Suzuki, K., Tokuhisa, T., Ohsumi, Y., and Yoshimori, T. (2001). Dissection of autophagosome formation using Apg5-deficient mouse embryonic stem cells. J. Cell Biol. *152*, 657–668.

Mizushima, N., Yamamoto, A., Matsui, M., Yoshimori, T., and Ohsumi, Y. (2004). In vivo analysis of autophagy in response to nutrient starvation using transgenic mice expressing a fluorescent autophagosome marker. Mol. Biol. Cell *15*, 1101–1111.

Nakatogawa, H., Ichimura, Y., and Ohsumi, Y. (2007). Atg8, a ubiquitin-like protein required for autophagosome formation, mediates membrane tethering and hemifusion. Cell *130*, 165–178.

Neuspiel, M., Schauss, A.C., Braschi, E., Zunino, R., Rippstein, P., Rachubinski, R.A., Andrade-Navarro, M.A., and McBride, H.M. (2008). Cargo-selected transport from the mitochondria to peroxisomes is mediated by vesicular carriers. Curr. Biol. *18*, 102–108.

Ogata, M., Hino, S., Saito, A., Morikawa, K., Kondo, S., Kanemoto, S., Murakami, T., Taniguchi, M., Tanii, I., Yoshinaga, K., et al. (2006). Autophagy is activated for cell survival after endoplasmic reticulum stress. Mol. Cell Biol. *26*, 9220–9231.

Overbye, A., Fengsrud, M., and Seglen, P.O. (2007). Proteomic analysis of membrane-associated proteins from rat liver autophagosomes. Autophagy *3*, 300–322.

Patterson, G.H., and Lippincott-Schwartz, J. (2002). A photoactivatable GFP for selective photolabeling of proteins and cells. Science *297*, 1873–1877.

Petiot, A., Ogier-Denis, E., Blommaart, E.F., Meijer, A.J., and Codogno, P. (2000). Distinct classes of phosphatidylinositol 3′-kinases are involved in signaling pathways that control macroautophagy in HT-29 cells. J. Biol. Chem. *275*, 992–998.

Petit, J.M., Maftah, A., Ratinaud, M.H., and Julien, R. (1992). 10N-nonyl acridine orange interacts with cardiolipin and allows the quantification of this phospholipid in isolated mitochondria. Eur. J. Biochem. *209*, 267–273.

Rajagopal, A., Rao, A.U., Amigo, J., Tian, M., Upadhyay, S.K., Hall, C., Uhm, S., Mathew, M.K., Fleming, M.D., Paw, B.H., et al. (2008). Haem homeostasis is regulated by the conserved and concerted functions of HRG-1 proteins. Nature *453*, 1127–1131.

Reef, S., Zalckvar, E., Shifman, O., Bialik, S., Sabanay, H., Oren, M., and Kimchi, A. (2006). A short mitochondrial form of p19ARF induces autophagy and caspase-independent cell death. Mol. Cell *22*, 463–475.

Reggiori, F., Shintani, T., Nair, U., and Klionsky, D.J. (2005). Atg9 cycles between mitochondria and the pre-autophagosomal structure in yeasts. Autophagy *1*, 101–109.

Reggiori, F., and Tooze, S.A. (2009). The EmERgence of autophagosomes. Dev. Cell *17*, 747–748.

Sakaki, K., Wu, J., and Kaufman, R.J. (2008). Protein kinase Ctheta is required for autophagy in response to stress in the endoplasmic reticulum. J. Biol. Chem. *283*, 15370–15380.

Sanjuan, M.A., Dillon, C.P., Tait, S.W., Moshiach, S., Dorsey, F., Connell, S., Komatsu, M., Tanaka, K., Cleveland, J.L., Withoff, S., and Green, D.R. (2007). Toll-like receptor signalling in macrophages links the autophagy pathway to phagocytosis. Nature *450*, 1253–1257.

Schmidt, K., and Nichols, B.J. (2004). A barrier to lateral diffusion in the cleavage furrow of dividing mammalian cells. Curr. Biol. *14*, 1002–1006.

Scott, S.V., Hefner-Gravink, A., Morano, K.A., Noda, T., Ohsumi, Y., and Klionsky, D.J. (1996). Cytoplasm-to-vacuole targeting and autophagy employ the same machinery to deliver proteins to the yeast vacuole. Proc. Natl. Acad. Sci. USA *93*, 12304–12308.

Sneve, M.L., Overbye, A., Fengsrud, M., and Seglen, P.O. (2005). Comigration of two autophagosome-associated dehydrogenases on two-dimensional polyacrylamide gels. Autophagy *1*, 157–162.

Tadini-Buoninsegni, F., Bartolommei, G., Moncelli, M.R., Tal, D.M., Lewis, D., and Inesi, G. (2008). Effects of high-affinity inhibitors on partial reactions, charge movements, and conformational States of the Ca^{2+} transport ATPase (sarco-endoplasmic reticulum Ca^{2+} ATPase). Mol. Pharmacol. *73*, 1134–1140.

Takagaki, Y., Radhakrishnan, R., Gupta, C.M., and Khorana, H.G. (1983). The membrane-embedded segment of cytochrome b5 as studied by cross-linking with photoactivatable phospholipids. J. Biol. Chem. *258*, 9128–9135.

Takahashi, Y., Coppola, D., Matsushita, N., Cualing, H.D., Sun, M., Sato, Y., Liang, C., Jung, J.U., Cheng, J.Q., Mul, J.J., et al. (2007a). Bif-1 interacts with Beclin 1 through UVRAG and regulates autophagy and tumorigenesis. Nat. Cell Biol. *9*, 1142–1151.

Takahashi, Y., Coppola, D., Matsushita, N., Cualing, H.D., Sun, M., Sato, Y., Liang, C., Jung, J.U., Cheng, J.Q., Mule, J.J., et al. (2007b). Bif-1 interacts with Beclin 1 through UVRAG and regulates autophagy and tumorigenesis. Nat. Cell Biol. *9*, 1142–1151.

Tasdemir, E., Galluzzi, L., Maiuri, M.C., Criollo, A., Vitale, I., Hangen, E., Modjtahedi, N., and Kroemer, G. (2008). Methods for assessing autophagy and autophagic cell death. Methods Mol. Biol. *445*, 29–76.

Thomas, P.D., and Poznansky, M.J. (1989). Curvature and composition-dependent lipid asymmetry in phosphatidylcholine vesicles containing phosphatidylethanolamine and gangliosides. Biochim. Biophys. Acta *978*, 85–90.

Tsukada, M., and Ohsumi, Y. (1993). Isolation and characterization of autophagy-defective mutants of Saccharomyces cerevisiae. FEBS Lett. *333*, 169–174.

van Meer, G., Voelker, D.R., and Feigenson, G.W. (2008). Membrane lipids: where they are and how they behave. Nat. Rev. Mol. Cell Biol. *9*, 112–124.

Vance, J.E. (2008). Phosphatidylserine and phosphatidylethanolamine in mammalian cells: two metabolically related aminophospholipids. J. Lipid Res. *49*, 1377–1387.

Vance, J.E., and Vance, D.E. (2004). Phospholipid biosynthesis in mammalian cells. Biochem. Cell Biol. *82*, 113–128.

Vergeres, G., and Waskell, L. (1995). Cytochrome b5, its functions, structure and membrane topology. Biochimie *77*, 604–620.

Xie, Z., and Klionsky, D.J. (2007). Autophagosome formation: core machinery and adaptations. Nat. Cell Biol. *9*, 1102–1109.

Ylä-Anttila, F., Vihinen, H., Jokitalo, E., and Eskelinen, E.L. (2009). 3D tomotgraphy redeals connections between the phagophore and endoplasmic reticulum. Autophagy *5*, 1180–1185.

Young, A.R., Chan, E.Y., Hu, X.W., Kochl, R., Crawshaw, S.G., High, S., Hailey, D.W., Lippincott-Schwartz, J., and Tooze, S.A. (2006). Starvation and ULK1-dependent cycling of mammalian Atg9 between the TGN and endosomes. J. Cell Sci. *119*, 3888–3900.

Yousefi, S., Perozzo, R., Schmid, I., Ziemiecki, A., Schaffner, T., Scapozza, L., Brunner, T., and Simon, H.U. (2006). Calpain-mediated cleavage of Atg5 switches autophagy to apoptosis. Nat. Cell Biol. *8*, 1124–1132.